Styrene-Butadiene Latex Blending as a Strategy to Mitigate Property Trade-offs in Paper Coatings

Jee-Hong Lee [a,†] and Hye Jung Youn [a,b,*]

Latex binders are the predominant binders in pigmented coatings for paper, and various latexes with different properties are selected depending on the target product. However, modifying latex binder properties to improve a particular coated paper property often introduces trade-offs in other properties. This study investigated the potential of latex blending to mitigate coated-paper property trade-offs compared with single-latex formulations, focusing on surface and optical properties, as well as ink absorption, and print-mottle-related behavior. Six styrene–butadiene (SB) latexes with different glass transition temperatures (T_g) and particle sizes were used, and coated paper property pairs exhibiting trade-off behavior were identified using single-latex formulations. Subsequently, coated papers were prepared with seven binary latex blends, and their trade-off performance relative to the single-latex formulations was evaluated using a trendline-based trade-off analysis. The results showed that low–high T_g blends provided improved trade-off performance compared with the single-latex formulations. The coexisting binder morphology in these blends enabled higher gloss with a smaller penalty in the trade-off properties, maintaining higher light-scattering efficiency and improving print-mottle-related behavior. The findings of this study indicate that latex blending has the potential to mitigate coated paper property trade-offs and provides a practical approach for optimizing coated paper performance.

DOI: 10.15376/biores.21.2.4180-4197

Keywords: Paper coating; Styrene-butadiene (SB) latex; Latex blending; Surface and optical properties; Print mottle; Trade-off analysis

Contact information: a: Department of Agriculture, Forestry and Bioresources, College of Agriculture and Life Sciences, Seoul National University, 1 Gwanak-ro, Gwanak-gu, Seoul 08826, Korea; b: Research Institute of Agriculture and Life Sciences, College of Agriculture and Life Sciences, Seoul National University, 1 Gwanak-ro, Gwanak-gu, Seoul 08826, Korea, Republic of Korea;
** Corresponding author: page94@snu.ac.kr; †: Present address: Namyang R&D Center, Hyundai Motor Company, 150, Hyundaiyeonguso-ro, Namyang-eup, Hwaseong-si, Gyeonggi-do, 18280*

INTRODUCTION

Pigmented coating is widely used to enhance the appearance and printability of paper and paperboard. This aqueous coating typically consists of mineral pigments, a polymeric binder, and functional additives, forming a porous coating layer on a base sheet. Because coating microstructure strongly governs coated-paper properties and is highly dependent on formulation, tailoring the coating formulation is essential for achieving desirable performance. Among formulation variables, the binder system is often adjusted to tailor coated-paper properties, and latex binders are among the most widely used binders in pigmented paper coatings. During drying and consolidation, latex particles redistribute

within the coating and deform/coalesce to form adhesive bridges and films, thereby bonding pigment–pigment and pigment–binder contacts (Watanabe and Lepoutre 1982; Keddie and Routh 2010; Zang *et al.* 2010). As a result, latex selection strongly influences coating microstructure development, which in turn affects coating strength as well as surface topography, optical properties, and ink–paper interactions relevant to printing (Lee 1997; Schmidt-Thümmes *et al.* 2009).

Among latex properties, glass transition temperature (T_g) and particle size are two frequently considered parameters. Latex T_g is closely related to particle deformability and film formation during drying. It therefore influences coating strength, micro-scale surface topography, and pore structure, thereby affecting ink uptake and printing performance (Lee 1997; Oh *et al.* 2019; Lee and Lee 2018, 2022a,b). Latex particle size may affect binder migration during drying, which can alter local binder distribution and properties within the coating layer, including near the surface (Zang *et al.* 2010; Lee *et al.* 2021). Particle size has also been reported to influence the mechanical integrity of the coating layer (Yoo *et al.* 2007; Okamoto 2020).

In practice, the tuning of latex T_g or particle size can improve one attribute while compromising another, resulting in trade-off relationships. For instance, higher T_g latexes can improve micro-scale surface smoothness and gloss by reducing coating shrinkage, yet limited deformation can reduce coating strength (Lee 1982; Groves *et al.* 1993; Schmidt-Thümmes *et al.* 2009). Similarly, smaller latex particles may enhance mechanical integrity through improved packing and bonding, but they may also be more susceptible to migration-driven inhomogeneity depending on formulation and drying conditions (Zang *et al.* 2010; Okamoto 2020; Shen *et al.* 2021). These coupled responses complicate binder selection and constrain simultaneous improvements in multiple end-use properties.

Blending different latexes may offer a practical strategy to address such trade-offs by providing complementary functions, as latex components with different properties can compensate for each other's limitations. A limited number of studies have reported benefits of latex blending in paper coating, such as improved rheological behavior using bimodal latex systems and improved mechanical integrity through incorporation of nano-sized latexes (Van Gilder and Lee 1983; Abhari *et al.* 2018; Shen *et al.* 2021). However, whether latex blending improves key surface-, optical-, and print-uniformity-related trade-offs relative to single-latex formulations has not been systematically investigated.

Accordingly, this study investigated the potential of latex blending to improve coated paper property trade-offs relative to single-latex formulations. Six styrene–butadiene (SB) latexes, a dominantly used binder for pigmented paper coatings, spanning a range of T_g and particle sizes were used. The authors first examined how latex T_g and particle size influence surface, optical, and ink-absorption/print-mottle-related properties in a simplified coating system. Trade-off pairs were then identified, and the performance of binary blends was quantified relative to single-latex formulations using a trendline-based trade-off analysis. The results provide practical guidance for binder selection and blending strategies in coated-paper design.

MATERIALS AND METHODS

Materials

A wood-free base paper (basis weight 108 ± 1 g/m2; Moorim P&P, Korea) was used. Ground calcium carbonate (GCC, Setacarb-77K, 98 wt% < 2 μm; Omya Korea Inc.,

Korea) was used as the coating pigment. Six SB latex binders were supplied by LG Chem, Ltd. (Korea), with varying glass-transition temperatures (T_g) and particle sizes (Table 1). Sodium carboxymethyl cellulose (CMC, Finnfix-5; CP Kelco, Korea) was used as a co-binder.

Table 1. (a) Classification of Latexes and (b) Properties. Latex Abbreviations Denote T_g-size (*e.g.*, LT-Sm = low-T_g, small).

(a)

T_g / Particle Size	Low-T_g	Mid-T_g	High-T_g
Small (≤120 nm)	LT-Sm	MT-Sm	—
Medium (121–150 nm)	LT-Md	MT-Md	—
Large (≥151 nm,)	LT-Lg	—	HT-Lg

(b)

	T_g (°C)	Particle Size (nm)	Gel Content (%)
LT-Sm	-5.0	122	77
LT-Md	-5.0	137	78
LT-Lg	-5.0	153	79
MT-Sm	10.0	110	85
MT-Md	10.0	150	75
HT-Lg	24.3	165	82

Coated Paper Preparation

The coating color consisted of ground calcium carbonate (GCC), a latex binder, and CMC. No additional additives were employed. The reason for not including other additives was to minimize interference from other formulation components and thereby isolate the effects of latex binder properties and binary blending. CMC (0.1 pph, based on the dry pigment weight) was dissolved in distilled water, followed by the addition of GCC. Subsequently, 12 pph of latex was incorporated into the mixture. The pH of the coating color was adjusted using 1 N sodium hydroxide (NaOH). Adequate mixing time was applied at each stage to ensure complete dispersion. The final solids content and pH of the coating color were 62% and 9.5, respectively.

The coating color was applied to the base paper using a laboratory auto rod coater (GIST, Korea) at a coating speed of 70 mm/s. The coated papers were then dried in a hot-air impingement dryer at 60 °C for 2 min and conditioned for 24 h at a constant temperature and relative humidity (25 °C, 50% RH). After conditioning, the samples were calendered twice using a soft-nip calender at a line speed of 10 m/min and a pressure of 143 kg/cm. All coated-paper properties presented in this study were measured using calendered samples, whereas the SEM observations in Figs. 4 and 7 were conducted on uncalendered coated papers.

Latex Compositions

Table 2 summarizes the latex compositions used in this study, including both the single-latexes and the binary blends. The binary blends refer to combinations of latexes differing in particle size or T_g. The selected binary blends were chosen to examine

representative blending cases involving particle size, T_g, and their combined effects, rather than to cover all possible binary combinations. To further examine the most extreme combined case, the blend ratio was varied for the low-high T_g-size cross blends. All blends were formulated with a fixed total latex dosage of 12 pph.

Table 2. Latex Compositions Used in This Study

Single-latex		
Low-T_g		LT-Sm
		LT-Md
		LT-Lg
Mid-T_g		MT-Sm
		MT-Md
High-T_g		HT-Lg
Binary Blends		
Size Blend (Low-T_g)		LT-Sm+LT-Lg (6:6)
Low-Mid T_g Blends		LT-Sm+MT-Md (6:6)
		LT-Lg+MT-Sm (6:6)
		LT-Lg+MT-Md (6:6)
Low-High T_g Blends	***Same-size blend (Large)***	LT-Lg+HT-Lg (6:6)
	T_g-size Cross Blends (Varying Ratio)	LT-Sm+HT-Lg (6:6)
		LT-Sm+HT-Lg (8:4)
		LT-Sm+HT-Lg (10:2)

Note: The blend ratios indicated in parentheses (e.g., 6:6, 8:4, and 10:2) denote the weight ratios of the two latexes in each binary blend, with the total latex dosage fixed at 12 pph.

Coated Paper Property Characterization

Surface and optical properties

Gloss, Parker Print-Surf (PPS) roughness, light scattering coefficient, light absorption coefficient, brightness, and opacity of the coated papers were evaluated. Gloss (TAPPI T480 (2015)) was measured at 75° using an L&W Gloss Meter (Lorentzen & Wettre, Sweden), based on 10 measurements. PPS roughness (TAPPI T555 (2015)) was determined using an L&W PPS Tester (Lorentzen & Wettre, Sweden), based on 5 measurements. Light scattering coefficient and light absorption coefficient (ISO 9416 (2009)), brightness (ISO 2470-1 (2016), and opacity (ISO 2471 (2008)) were measured using an L&W Elrepho spectrophotometer (Lorentzen & Wettre, Sweden), based on 3 measurements.

Ink absorption properties and print mottle assessment

Three laboratory tests were conducted to evaluate the ink absorption and print mottle behavior of the coated papers: Croda ink absorption, ink vehicle absorption uniformity, and back-trapping simulation. All ink absorption and print mottle tests were conducted in triplicate.

The Croda ink absorption test applies a uniform ink film and allows sufficient penetration time, excluding nip-related dynamics (film splitting, retransfer, picking). It therefore probes deeper-layer absorption uniformity, independent of press conditions, and provides a complementary diagnostic to dynamic printing tests. The ink vehicle absorption uniformity test is carried out using a rotary ink (RI) tester (RI-3, Akira, Japan; Fig. 1a), where the ink vehicle (Dongyang Ink, Korea) is applied to the first blanket roll and the IGT mottle test ink (IGT Testing Systems, Netherlands) is continuously printed from the second roll. This procedure characterizes near-surface absorption uniformity over a limited dwell time under nip conditions. The back-trapping simulation test uses the RI tester to mimic the back-trapping phenomenon during printing. The IGT mottle test ink is first applied with the initial blanket roll and then re-transferred to a clean second blanket roll. This test provides the highest process fidelity among the three methods.

The Croda ink absorption test was performed according to SCAN P70:09 (2009), and the Croda ink absorbency value and its absorption uniformity were evaluated. Croda ink, composed of a colorless pigment and a red vehicle, was applied at a thickness of 25 μm using a four-sided film applicator. After a 2-minute absorption time, excess ink was removed.

Ink absorbency value was calculated using the luminance factor (ISO 2471 (2008)) of the coated paper and of the ink-stained coated paper, following SCAN-P 70:09 (2009) (Eq. 1). This parameter represents the relative amount of ink absorbed by the coated paper,

$$A = \frac{100 \cdot (R_\infty - R_y)}{R_\infty} \quad (1)$$

where A is the ink absorbency value, R_∞ is the intrinsic luminance factor of the coated paper, and R_y is the luminance factor of the ink-stained area, both determined according to ISO 2471 (2008) over an opaque pad of the coated paper.

Croda ink absorption uniformity was assessed by determining the mottle index of the Croda ink–stained papers. This parameter reflects the spatial uniformity of ink penetration across the coated surface, with lower mottle index values indicating more uniform absorption. The stained samples were scanned using an Epson Perfection V33 scanner, and the mottle index (spatial wavelength: 1–8 mm) was calculated using the STFI Mottling Expert v1.31 software.

Ink vehicle absorption uniformity (Fig. 1b) was evaluated using the RI tester. A 0.20 mL of ink vehicle and 0.20 mL of IGT mottle test ink were applied to the first and second blanket rolls, respectively, each producing a 1.70 μm film thickness on the blanket. The coated papers were then printed continuously, and the final prints were scanned using an Epson Perfection V33 scanner. The mottle index (spatial wavelength: 1 to 8 mm) was calculated using the STFI Mottling Expert v1.31 software.

The back-trapping simulation test (Fig. 1c) was performed using the RI tester. A 0.14 mL of IGT mottle test ink was applied to the first blanket roll, corresponding to a film thickness of 1.22 μm on the blanket roll. The second blanket roll was a clean, uninked roll. The coated papers were then printed continuously, and the final prints were scanned using an Epson Perfection V33 scanner. The mottle index (wavelength range: 1 to 8 mm) was calculated using the STFI Mottling Expert v1.31 software.

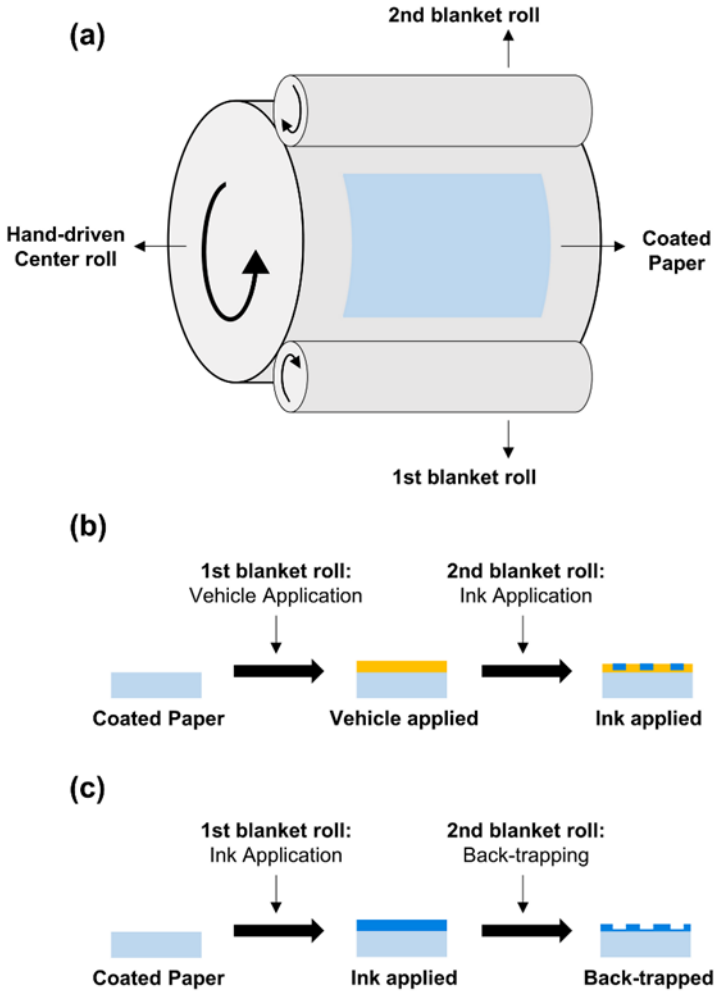

Fig. 1. Schematics of the RI tester and laboratory tests used to evaluate ink absorption and print mottle behavior. Schematic of (a) the RI tester (hand-driven center roll with two blanket rolls), (b) ink–vehicle absorption uniformity test (1st blanket roll: vehicle; 2nd blanket roll: ink application), (c) Back-trapping simulation test (1st blanket roll: ink; 2nd blanket roll: clean blanket roll)

Trade-off analysis

To assess the benefits of using binary latex blend formulations over single-latex binders, a trade-off analysis was conducted, as illustrated in Fig. 2. Pairs of properties exhibiting a trade-off relationship were selected based on the observed influence of latex properties on the coated paper properties (Table 3). In practical terms, this analysis examines whether blending shifts a formulation to a more favorable position than the baseline trade-off defined by the single-latex systems. A positive deviation from the single-latex trendline therefore indicates mitigation of the trade-off.

A trendline was fitted using the data obtained from the single-latex formulations, and the orthogonal distance of each binary blend from this trendline was calculated. The trade-off improvement rank was then determined based on the magnitude of the orthogonal distance in the direction of property improvement.

For trendline fitting, only first- and second-order polynomial models were considered to avoid overfitting. A linear model was preferred; however, a quadratic model was selected when the adjusted R^2 increased by more than 0.02 and the residuals exhibited systematic curvature. While this approach provides a practical and consistent basis for

comparative evaluation, it should be noted that the ranking may depend to some extent on the fitting model and distance metric adopted. Therefore, the trade-off results in this study should be interpreted as comparative trends within the present analytical framework.

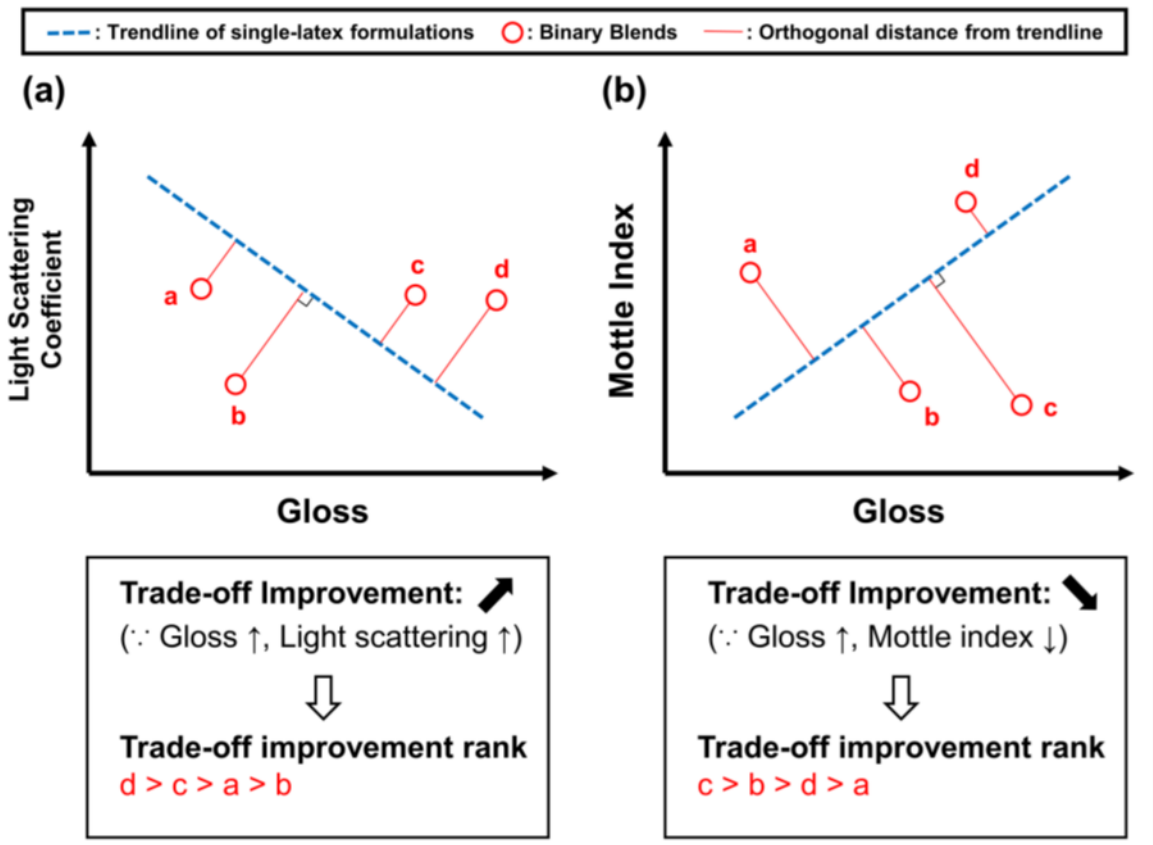

Fig. 2. Schematic illustration of the trade-off analysis with two examples: (a) light-scattering coefficient vs. gloss and (b) mottle index vs. gloss. The two examples represent the two improvement-direction patterns in this study. For (a), an increase in gloss (x-axis) and an increase in the light-scattering coefficient (y-axis) indicate improvement; for (b), an increase in gloss (x-axis) and a decrease in the mottle index (y-axis) indicate improvement. The dashed blue line is the trendline obtained from single-latex formulations, and red circles indicate binary-blend formulations. The red solid lines denote the orthogonal distances from the trendline. The trade-off improvement rank was determined based on the magnitude of the orthogonal distance in the direction of property improvement.

RESULTS AND DISCUSSION

Single-latex Formulation: Influence of Latex T_g and Particle Size

Surface and optical properties

Figure 3 shows the gloss and Parker Print-Surf (PPS) roughness of coated papers prepared with single-latex formulations. The gloss increased with higher latex T_g, whereas PPS roughness was independent of latex properties. This increase in gloss was particularly pronounced for coatings containing high-T_g latex. Gloss is an indicator of the micro-scale roughness of a coating surface, while PPS roughness, measured by an air-leakage method, reflects roughness at larger length scales (Xu *et al.* 2005; Järnström *et al.* 2008). These results therefore indicate that the latex T_g affected the micro-roughness of the coating, but

not to the large-scale surface roughness. It has been reported that high-T_g latex binders reduce coating shrinkage during drying, resulting in a smoother and consequently glossier surface (Lee 1982; Groves *et al.* 1993), which is consistent with these observations. Latex particle size did not exhibit measurable effects on either gloss or PPS roughness.

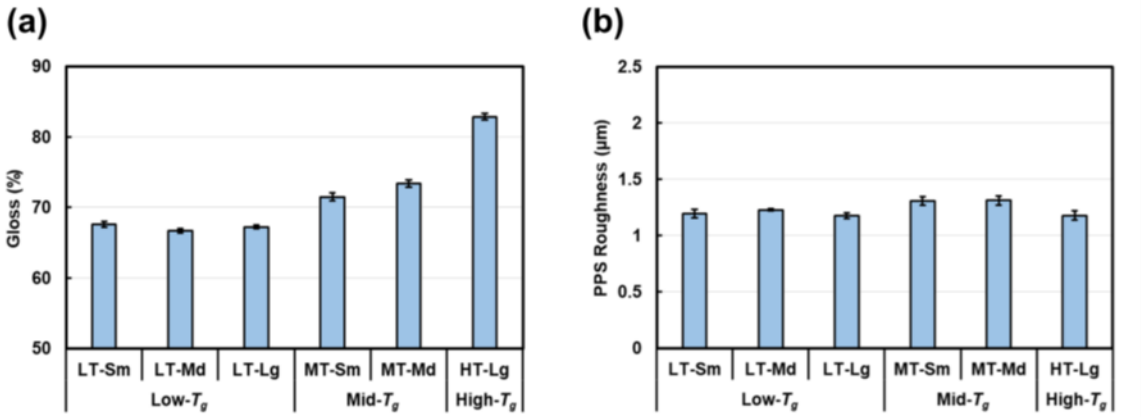

Fig. 3. (a) Gloss and (b) Parker Print-Surf (PPS) roughness of coated papers prepared with single-latex formulations

Figure 4 presents the light scattering coefficient, absorption coefficient, brightness, and opacity of coated papers prepared with single-latex formulations. The light scattering coefficient decreased with increasing latex T_g. The absorption coefficient showed similar values for coatings containing low- and mid-T_g latexes but increased for those containing high-T_g latex. A similar trend was observed for brightness, which remained nearly constant for coatings with low- and mid-T_g latexes but decreased for coatings containing high-T_g latex. In contrast, the opacity remained essentially unchanged regardless of the latex properties. Latex particle size did not influence any of the optical properties.

The light scattering coefficient is known to be strongly governed by the specific surface area and pore structure of the coating layer (Farnood 2009). In related studies by our group, higher T_g latexes were shown to produce a finer coating pore structure (Lee and Lee 2018; Lee and Lee 2022b). The coating structural change exhibited a sharp, threshold-like transition when plotted against latex deformation (Lee and Lee 2022a,b; Lee *et al.* 2022). In the fine-GCC (98 wt% < 2 μm) coating systems examined in these studies, the average pore size was already smaller than 0.2 μm even for the low-T_g latex. Because the optimal pore size for maximizing the light scattering efficiency of GCC-based coatings is approximately 0.2 μm (Gane *et al.* 2009), this implies that further pore refinement inevitably leads to a reduction in the light scattering coefficient.

Accordingly, the present results can be interpreted as follows. The use of higher T_g latex produced a finer pore structure, which in turn reduced the light scattering coefficient. When compared with the low-T_g latex system, this pore structure modification was substantially more pronounced for the high-T_g latex systems, whereas only minor changes are expected for the mid-T_g latex systems. As a consequence, both the absorption coefficient and brightness decreased for the high-T_g latex systems, while the mid-T_g latex systems exhibited optical properties comparable to those of the low-T_g latex systems.

SEM observations supported this interpretation (Fig. 4e-g), showing that the high-T_g latex particles remained largely spherical with limited deformation, whereas the low- and mid-T_g latexes underwent substantial deformation, forming continuous films. These differences in latex deformation behavior are likely to induce pronounced differences in

the coating pore structure. The similar opacity values observed for all coated papers are attributed to the high basis weight and coating weight, which govern the overall sheet opacity regardless of variations in the coating microstructure.

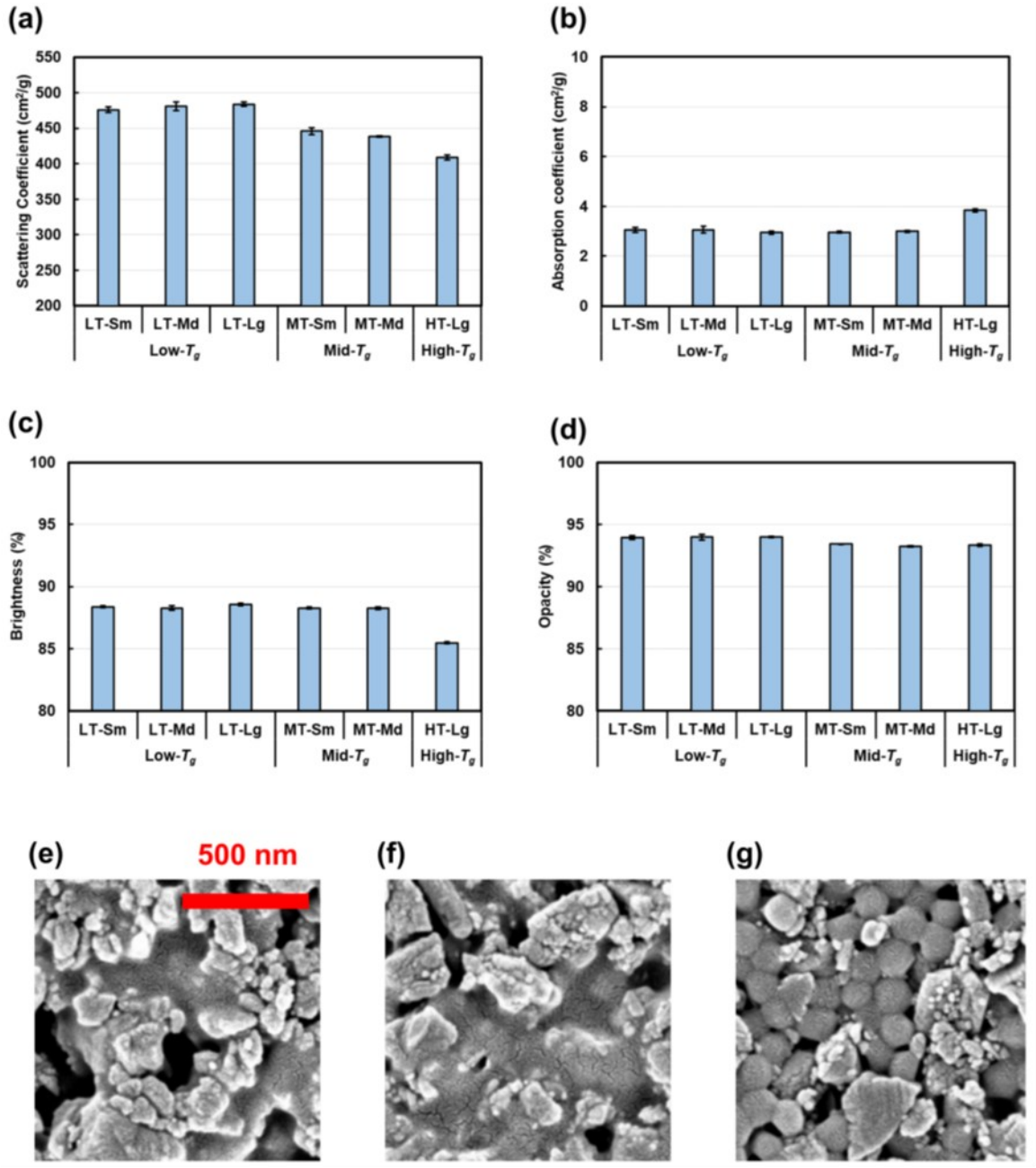

Fig. 4. (a) Light scattering coefficient, (b) light absorption coefficient, (c) brightness, and (d) opacity of coated papers prepared with single-latex formulations. (e–g) Surface SEM images of the coating layers on the uncalendered coated papers prepared with single-latex formulations: (e) LT-Lg, (f) MT-Sm, and (g) HT-Lg

Ink absorption and print-mottle-related behavior

Figure 5 shows the ink absorption and print mottle behavior of the coated papers. Croda ink absorbency increased with increasing latex T_g. The Croda ink absorption non-uniformity also increased with higher T_g latexes, and the high-T_g latex system in particular

exhibited a markedly high mottle index. In the vehicle absorption and back-trapping tests, coated papers containing the high-T_g latex could not be evaluated due to severe picking, indicating insufficient coating strength. In the vehicle absorption test, the mid-T_g latex systems exhibited higher mottle indices than the low-T_g latex systems. In the back-trapping test, the mid-T_g small-particle-size latex showed a higher mottle index than the low-T_g latex system, whereas the mid-T_g medium-particle-size latex exhibited a mottle index comparable to that of the low-T_g latex system. Regarding latex particle size, no consistent overall trend was detected.

The finer pore structure induced by the higher T_g latex formulation led to faster ink absorption, as capillary-driven transport is the dominant driving force for ink setting in offset printing (Rousu *et al.* 2003; Ström 2005). The non-uniform ink absorption observed for the high-T_g latex systems is consistent with reports in the literature that high-T_g latex formulations induce less uniform ink uptake (Purfeerst and Van Gilder 1991; Branston and Hobbs 1998; Lee and Lee 2018).

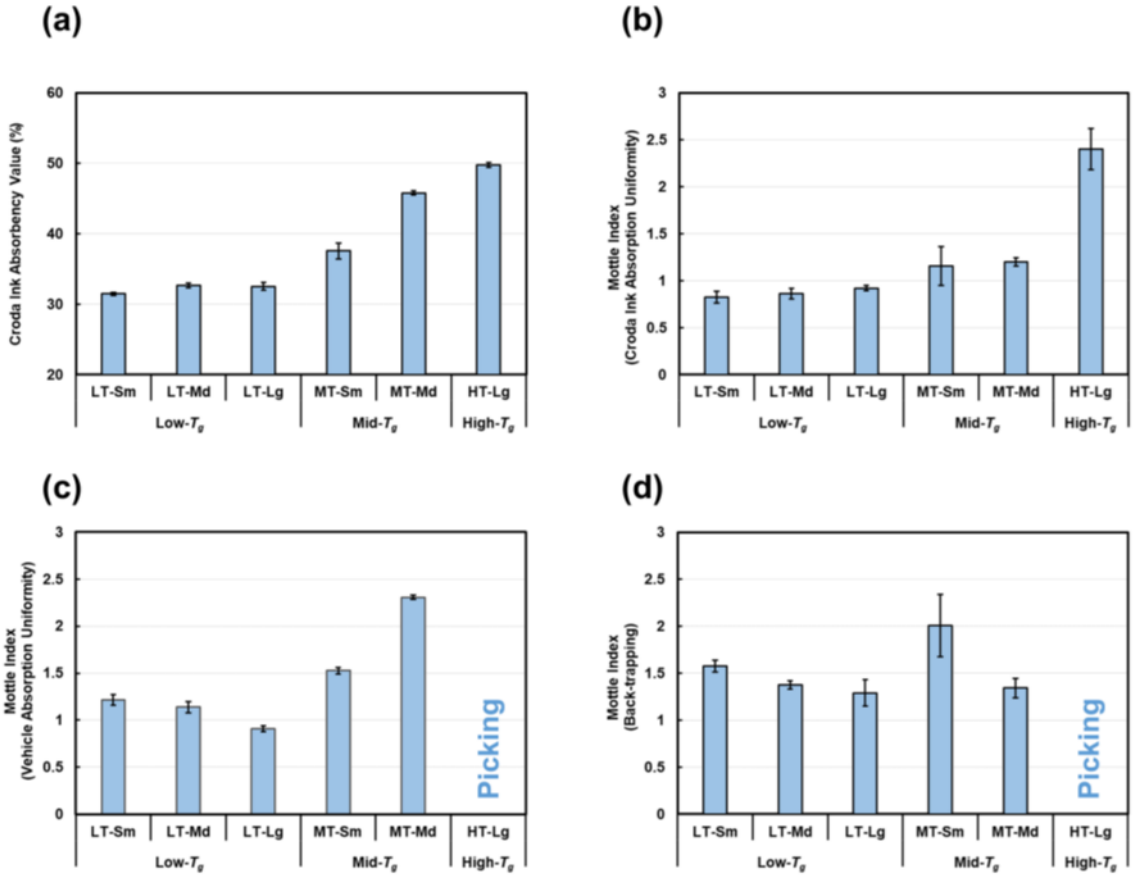

Fig. 5. (a) Croda ink absorbency, (b) Croda ink absorption uniformity, (c) offset ink vehicle absorption uniformity, and (d) back-trapping mottle index of coated papers prepared with single-latex formulations

Table 3 summarizes the influence of latex T_g and particle size on the properties of coated papers prepared with single-latex formulations. The latex T_g had a marked influence on the coated paper properties. The difference was especially pronounced for the high-T_g latex system due to the threshold-like structural transition associated with latex deformation. The major benefit of using high-T_g latex was the increased gloss; however,

the light-scattering coefficient, absorption coefficient, brightness, and ink-absorption uniformity deteriorated as a trade-off. In addition, the severe picking observed for the high-T_g formulation indicated reduced coating strength. With respect to latex particle size, no noticeable influence on the coated paper properties was observed in the present study.

Table 3. Summary of the Effects of Increasing Latex T_g and Particle Size on the Properties of Coated Papers

Property	Higher T_g	Larger Particle Size
Gloss	↑	—
PPS Roughness	—	—
Light Scattering Coefficient	↓	—
Light Absorption Coefficient	↑ (High-T_g only)	—
Brightness	↓ (High-T_g only)	—
Opacity	—	—
Croda Ink Absorbency	↑	—
Croda Ink Absorption Uniformity	↓	±
Ink Vehicle Absorption Uniformity	↑ (Low-Mid T_g)	±
Back-trapping Mottle	± (Low-Mid T_g)	±

Notes: (↑, increase; ↓, decrease; —, no noticeable change; ±, inconsistent). Ink vehicle absorption uniformity and the back-trapping simulation test could not be evaluated for the high-T_g latex systems because severe picking occurred.

Binary Blends: Trade-off Analysis

Trade-offs between gloss and optical properties

Figure 6 presents the trade-off analysis between gloss and the light-scattering coefficient, brightness, and light-absorption coefficient. For light-scattering coefficient, size-blends (low-T_g) and low–mid T_g blends showed no substantial deviation from the single-latex trendline, indicating that blending did not improve the gloss–scattering trade-off relative to the single-latex formulation. In contrast, low–high T_g blends increased gloss without a pronounced loss in scattering: the scattering coefficient remained above 450 cm²/g, exceeding that of mid-T_g single-latex formulations.

Regarding brightness and the absorption coefficient, all binary blends showed minimal deviation from the single-latex trendline. They remained near the low- and mid-T_g single-latex levels, with no noticeable change in either property. Although the high-T_g single-latex formulation exhibited lower brightness and a higher absorption coefficient than the low-T_g formulation, blending with low-T_g latex maintained both properties at levels comparable to the low-T_g single-latex system. The results indicated that low–high T_g binary blends can improve the surface and optical properties by improving light-scattering–gloss trade-off relative to the single-latex formulations.

These results suggest that a coexisting binder morphology (Fig. 7), in which the low-T_g latex forms a continuous film while the high-T_g latex remains less deformed and more particulate, can provide complementary functions and be advantageous relative to a single-latex binder morphology. Enhanced film formation by the deformable low-T_g latex,

in combination with the reduced fraction of high-T_g latex in the blends (a 50 to 84% decrease relative to the high-T_g single-latex formulation for 6:6, 8:4, and 10:2 ratios), is expected to moderate the development of an excessively fine coating pore structure and thereby maintain higher scattering efficiency. At the same time, the incorporated high-T_g latex can reduce coating shrinkage and improve micro-scale surface smoothness; gloss also increased with increasing high-T_g latex fraction. This combination therefore provides a more favorable gloss–light-scattering balance.

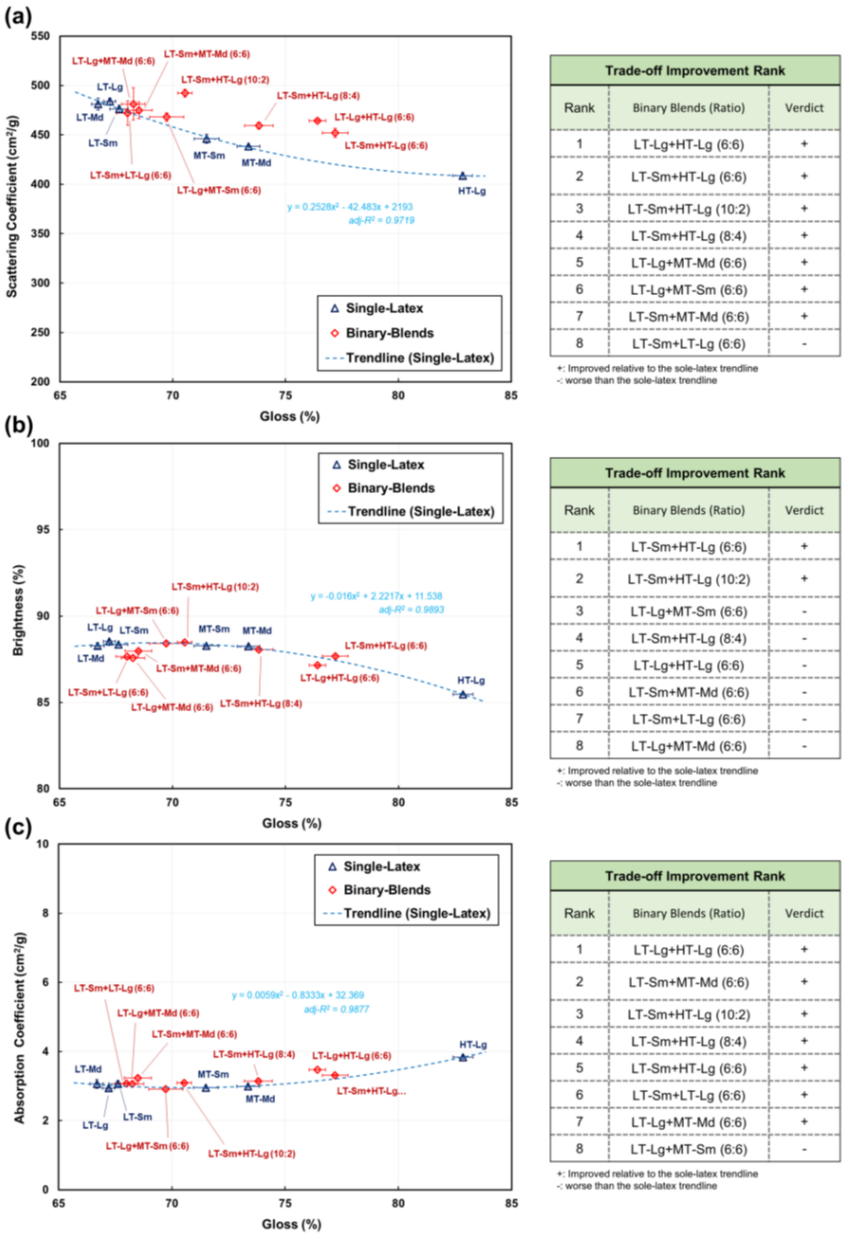

Trade-off Improvement Rank

Rank	Binary Blends (Ratio)	Verdict
1	LT-Lg+HT-Lg (6:6)	+
2	LT-Sm+HT-Lg (6:6)	+
3	LT-Sm+HT-Lg (10:2)	+
4	LT-Sm+HT-Lg (8:4)	+
5	LT-Lg+MT-Md (6:6)	+
6	LT-Lg+MT-Sm (6:6)	+
7	LT-Sm+MT-Md (6:6)	+
8	LT-Sm+LT-Lg (6:6)	-

+: Improved relative to the sole-latex trendline
-: worse than the sole-latex trendline

Trade-off Improvement Rank

Rank	Binary Blends (Ratio)	Verdict
1	LT-Sm+HT-Lg (6:6)	+
2	LT-Sm+HT-Lg (10:2)	+
3	LT-Lg+MT-Sm (6:6)	-
4	LT-Sm+HT-Lg (8:4)	-
5	LT-Lg+HT-Lg (6:6)	-
6	LT-Sm+MT-Md (6:6)	-
7	LT-Sm+LT-Lg (6:6)	-
8	LT-Lg+MT-Md (6:6)	-

+: Improved relative to the sole-latex trendline
-: worse than the sole-latex trendline

Trade-off Improvement Rank

Rank	Binary Blends (Ratio)	Verdict
1	LT-Lg+HT-Lg (6:6)	+
2	LT-Sm+MT-Md (6:6)	+
3	LT-Sm+HT-Lg (10:2)	+
4	LT-Sm+HT-Lg (8:4)	+
5	LT-Sm+HT-Lg (6:6)	+
6	LT-Sm+LT-Lg (6:6)	+
7	LT-Lg+MT-Md (6:6)	+
8	LT-Lg+MT-Sm (6:6)	-

+: Improved relative to the sole-latex trendline
-: worse than the sole-latex trendline

Fig. 6. Trade-off analysis between gloss and (a) the light-scattering coefficient, (b) brightness, and (c) light-absorption coefficient. The trendline for the single-latex formulations is shown as a blue dashed line; single-latex data are shown as blue triangles and binary blends as red diamonds. The tables summarize the trade-off improvement rank of the binary blends relative to the single-latex trendline (+, improved; −, worsened).

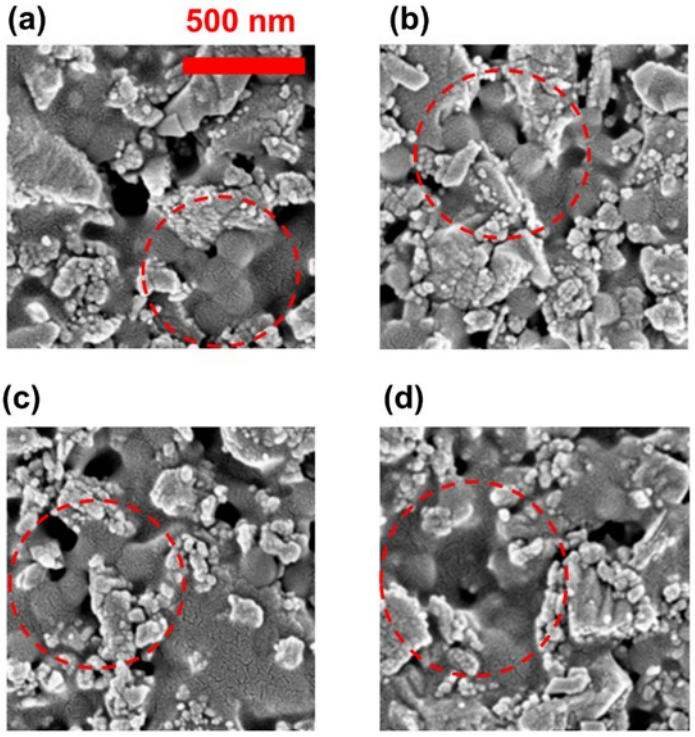

Fig. 7. Surface SEM images of the coating layers on uncalendered coated papers prepared with low–high T_g blends: (a) LT-Lg + HT-Lg (6:6), (b) LT-Sm + HT-Lg (6:6), (c) LT-Sm + HT-Lg (8:4), and (d) LT-Sm + HT-Lg (10:2). Red dashed circles indicate regions where the coexisting binder morphology is clearly visible.

Trade-offs between gloss and print-mottle-related properties

Figure 8 presents the trade-off analysis between gloss and Croda ink absorption uniformity, ink vehicle absorption uniformity, and the mottle index derived from the back-trapping simulation. For the 6:6 low–high T_g blends, severe picking occurred, preventing evaluation of the ink vehicle absorption uniformity and back-trapping simulation–derived mottle index. The high fraction of high-T_g latex led to insufficient coating strength. For Croda ink absorption uniformity, most binary blends showed no substantial deviation from the single-latex trendline, except for LT-Lg+MT-Sm (6:6), LT-Lg+MT-Md (6:6), and LT-Lg+HT-Lg (6:6), which exhibited higher mottle indices than expected from the trendline. These results suggest that binary blending did not improve long-timescale, static uptake uniformity and, in some cases, even worsened it.

In contrast, the ink vehicle absorption uniformity results showed that most binary blends deviated toward lower mottle indices relative to the single-latex trendline, indicating improved behavior under nip-driven conditions, except for LT-Sm+LT-Lg (6:6) and LT-Lg+MT-Sm (6:6), both of which remained close to the trendline. The low–high T_g blends (8:4 and 10:2) exhibited the most favorable deviations from the single-latex trendline. Because the back-trapping simulation results for the single-latex formulations did not show a consistent trend (Fig. 5d), fitting a reliable single-latex trendline was not straightforward. Given that the higher T_g single-latex formulations consistently exhibited higher mottle indices in both the Croda ink absorption uniformity and ink vehicle absorption uniformity tests, the trendline in Fig. 8c was fitted after excluding the mid- T_g large-latex data point, which behaved as an apparent outlier. The interpretation of the back-trapping trade-off is therefore discussed under this assumption. The back-trapping simulation results showed

improvements similar to those observed in the ink vehicle absorption uniformity test. Although the deviations were smaller, most binary blends still shifted toward lower mottle indices, with the low–high T_g blends (8:4 and 10:2) showing the greatest improvement. The gloss-mottle trade-off analyses indicate that low–high T_g blending can improve print-mottle-related performance at a given gloss relative to the single-latex formulations.

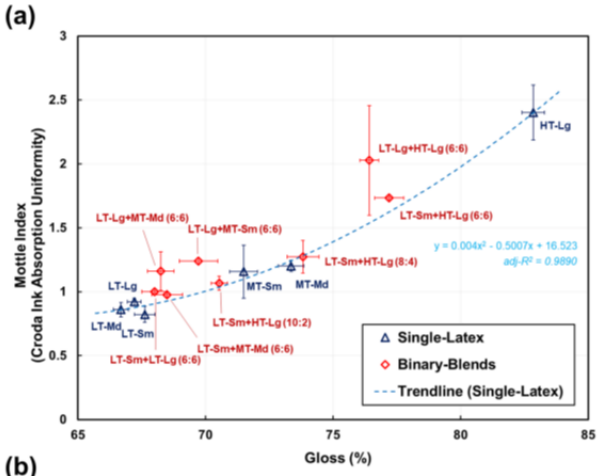

Trade-off Improvement Rank		
Rank	Binary Blends (Ratio)	Verdict
1	LT-Sm+HT-Lg (8:4)	+
2	LT-Sm+HT-Lg (10:2)	-
3	LT-Sm+MT-Md (6:6)	-
4	LT-Sm+LT-Lg (6:6)	-
5	LT-Sm+HT-Lg (6:6)	-
6	LT-Lg+MT-Md (6:6)	-
7	LT-Lg+MT-Sm (6:6)	-
8	LT-Lg+HT-Lg (6:6)	-

+: Improved relative to the sole-latex trendline
-: worse than the sole-latex trendline

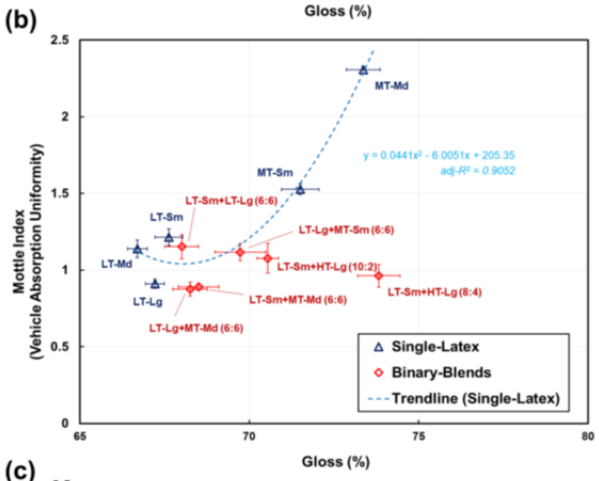

Trade-off Improvement Rank		
Rank	Binary Blends (Ratio)	Verdict
1	LT-Sm+HT-Lg (8:4)	+
2	LT-Sm+HT-Lg (10:2)	+
3	LT-Lg+MT-Md (6:6)	+
4	LT-Sm+MT-Md (6:6)	+
5	LT-Lg+MT-Sm (6:6)	-
6	LT-Sm+LT-Lg (6:6)	-
N/A	LT-Lg+HT-Lg (6:6)	Picking
N/A	LT-Sm+HT-Lg (6:6)	Picking

+: Improved relative to the sole-latex trendline
-: worse than the sole-latex trendline

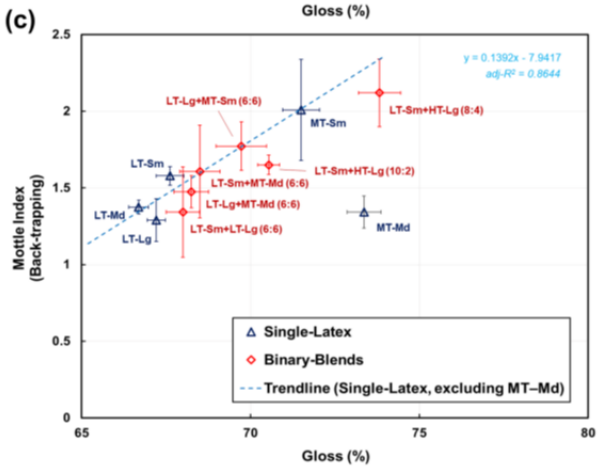

Trade-off Improvement Rank		
Rank	Binary Blends (Ratio)	Verdict
1	LT-Sm+HT-Lg (10:2)	+
2	LT-Sm+HT-Lg (8:4)	+
3	LT-Sm+LT-Lg (6:6)	+
4	LT-Lg+MT-Md (6:6)	+
5	LT-Lg+MT-Sm (6:6)	-
6	LT-Sm+MT-Md (6:6)	-
N/A	LT-Lg+HT-Lg (6:6)	Picking
N/A	LT-Sm+HT-Lg (6:6)	Picking

+: Improved relative to the sole-latex trendline
-: worse than the sole-latex trendline

Fig. 8. Trade-off analysis between gloss and (a) Croda ink absorption uniformity, (b) ink vehicle absorption uniformity, and (c) the mottle index derived from the back-trapping simulation. Severe picking occurred for the 6:6 low–high T_g blends in the tests shown in (b) and (c); therefore, the corresponding data are not shown. The trendline in (c) was fitted using the single-latex data excluding MT-Md. Symbols and tables follow the same definitions as in Fig. 6.

The results suggest that the coexisting binder morphology in low–high T_g blends can also be beneficial for ink absorption uniformity under nip-driven conditions, particularly near the coating surface. The Croda ink absorption uniformity test probes static uptake over a longer timescale using a relatively low-viscosity fluid and therefore is likely more sensitive to through-thickness transport heterogeneity (*i.e.*, the bulk pore network and connectivity). The Croda results showed no improvement in absorption uniformity for the binary blends, suggesting that long-timescale, through-thickness uptake uniformity across the coating layer remained largely unchanged. In contrast, the ink vehicle absorption and back-trapping tests probe uptake on short timescales and ink transfer/splitting under nip-driven contact, where near-surface pore-entry characteristics, real contact area, and mechanical integrity of the coating layer can play a stronger role. Accordingly, even if low–high T_g blends do not improve long-timescale, bulk uptake uniformity, they may still enhance nip-relevant uniformity by promoting smoother micro-scale surface topography and more stable transfer/splitting during the short dwell time in the nip.

Overall trade-off assessment of binary blends

The trade-off analysis indicated that low–high T_g blends provided the most favorable balance among gloss, optical properties, and print-mottle-related behavior. This improvement is likely due to the combination of the gloss benefit of the high-T_g latex and the enhanced film-forming ability of the low-T_g latex. The results also suggested that using a high-T_g latex as a sole binder is limited despite its gloss benefit, because it reduces coating strength and deteriorates other properties. In contrast, blending low- and high-T_g latexes provides a practical strategy for paper manufacturers to optimize coated-paper properties.

Regarding latex particle size, no noticeable effects were observed on the measured coated-paper properties in this study, and particle-size blends therefore appeared to provide limited benefit under the present experimental conditions. However, this should not be interpreted as evidence that particle size plays a negligible role, as this result may reflect the specific experimental conditions investigated here. For instance, the particle size range used in this study (110–165 nm) may have been too narrow to show a significant influence of particle size. Latex particle size may still influence coating structure and performance, such as binder distribution and the mechanical integrity of the coating layer (Lee 1997; Yoo *et al.* 2007; Zang *et al.* 2010; Okamoto 2020). Accordingly, further investigation may be needed to clarify the potential benefits of particle-size blending.

CONCLUSIONS

1. Single-latex formulation analysis clarified trade-offs among coated paper properties with respect to latex glass transition temperature (T_g) and particle size. Latex T_g increased gloss; however, light-scattering coefficient, absorption coefficient, brightness, and ink-absorption uniformity deteriorated as a trade-off. Within the experimental conditions investigated in this study, latex particle size had no measurable influence on the coated-paper properties evaluated.
2. Low-high T_g latex blends, representing a coexisting binder morphology, improved trade-off performance in both gloss–light-scattering efficiency and gloss–print-mottle-related behavior relative to the single-latex formulations. Specifically, these blends achieved higher gloss while maintaining higher light-scattering efficiency and more

favorable print-mottle-related characteristics than predicted from the single-latex trendlines, indicating a reduced trade-off penalty.

3. The high T_g latex induced severe picking issue due to insufficient coating strength, indicating that its use as a sole binder is limited. However, trade-off analysis suggests that incorporating a high-T_g latex in a blended binder system can mitigate the drawbacks of the high-T_g latex alone while retaining its gloss benefit.

ACKNOWLEDGMENTS

This work was supported by LG Chem.

Conflict of Interest

All authors declare that they have no known competing financial interests or personal relationships that could have appeared to influence the work reported in this paper.

REFERENCES CITED

Abhari, A. R., Shen, Z., Im, W., Lee, J. H., Kwon, S., and Lee, H. L. (2018). "Characteristics of suspension-polymerized latex and its effect on coated paper properties," *Journal of Korea TAPPI* 50(4), 149-155. https://doi.org/10.7584/JKTAPPI.2018.08.50.4.149

Branston, R. E., and Hobbs, D. G. (1998). "Styrene-butadiene latices," in: *Synthetic Coating Adhesives*, A. MacNair (ed.), TAPPI Press, Atlanta, GA, USA, pp. 1-17.

Farnood, R. (2009). "Optical properties of paper: Theory and practice," in: *Advances in Pulp and Paper Research: Transactions of the XIVth Fundamental Research Symposium*, Manchester, UK, pp. 273-352. https://doi.org/10.15376/frc.2009.1.273

Gane, P. A. C., Huggenberger, L., Arnold, M., and Köster, H. (2009). "Ground calcium carbonate," in: *Pigment Coating and Surface Sizing of Paper (Papermaking Science and Technology*, J. Paltakari (ed.), Fapet Oy, Helsinki, Finland, pp. 98-109.

Groves, R., Penson, J. E., and Ruggles, C. (1993). "Styrene-butadiene latex binders and coating structure," in: *TAPPI Coatings Conference Proceedings*, Minneapolis, MN, USA.

ISO 2471 (2008). "Paper and board — Determination of opacity (paper backing) — Diffuse reflectance method," International Organization for Standardization, Geneva, Switzerland.

ISO 9416 (2009). "Paper — Determination of light scattering and absorption coefficients (using Kubelka-Munk theory)," International Organization for Standardization, Geneva, Switzerland.

ISO 2470-1 (2016). "Paper, board and pulps — Measurement of diffuse blue reflectance factor — Part 1: Indoor daylight conditions (ISO brightness)," International Organization for Standardization, Geneva, Switzerland.

Järnström, J., Ihalainen, P., Backfolk, K., and Peltonen, J. (2008). "Roughness of pigment coatings and its influence on gloss," *Applied Surface Science* 254(18), 5741-5749. https://doi.org/10.1016/j.apsusc.2008.03.043

Keddie, J., and Routh, A. F. (2010). *Fundamentals of Latex Film Formation: Processes*

and Properties, Springer Science & Business Media. https://doi.org/10.1007/978-90-481-2845-7

Lee, D. I. (1982). "Development of high-gloss paper coating latexes," in: *TAPPI Coatings Conference Proceedings*, San Francisco, CA, USA, pp. 125-135.

Lee, D. I. (1997). "Latex applications in paper coating," in: *Polymeric Dispersions: Principles and Applications*, Springer Netherlands, Dordrecht, The Netherlands, pp. 497-513. https://doi.org/10.1007/978-94-011-5512-0_32

Lee, H. L., Youn, H. J., He, M., and Chen, J. (2021). "Back-trap mottle: A review of mechanisms and possible solutions," *BioResources* 16(3), 6426-6447. https://doi.org/10.15376/biores.16.3.lee

Lee, J. H., and Lee, H. L. (2018). "Characterization of the paper coating structure using focused ion beam and field-emission scanning electron microscopy. 2. Structural variation depending on the glass transition temperature of an S/B latex," *Industrial & Engineering Chemistry Research* 57(49), 16718-16726. https://doi.org/10.1021/acs.iecr.8b04802

Lee, J. H., and Lee, H. L. (2022a). "Novel method for the evaluation of mechanical property of pigment coating layer and its application: Influence of spreading of latex binder on final properties of coating layer," *Progress in Organic Coatings* 163, article 106652. https://doi.org/10.1016/j.porgcoat.2021.106652

Lee, J. H., and Lee, H. L. (2022b). "Quantitative analysis of the pigment coating structure influenced by the spreading of latex binder: In situ analysis of correlations between different structural properties," *Progress in Organic Coatings* 165, article 106739. https://doi.org/10.1016/j.porgcoat.2022.106739

Lee, J. H., Shin, S. J., Yeu, S. U., and Lee, H. L. (2022). "Quantitative characterization of the spreading and adhesion of styrene-butadiene latex binder in the dried pigment coating layer," *Progress in Organic Coatings* 162, article 106555. https://doi.org/10.1016/j.porgcoat.2021.106555

Oh, K., Rajabi Abhari, A., Im, W., Lee, J.-H., Shen, Z., Kwon, S., Yeu, S. U., and Lee, H. L. (2019). "Effect of core-shell structure latex on pigment coating properties," *BioResources* 14(1), 1241-1251. https://doi.org/10.15376/biores.14.1.1241-1251

Okamoto, N. (2020). "Application of SEM observation on coating layer for latex binder improvement," *Japan TAPPI Journal* 74(4), 401-405. https://doi.org/10.2524/jtappij.74.401

Purfeerst, R. D., and Van Gilder, R. L. (1991). "Tail-edge picking, back-trap mottle and fountain solution interference of model latex coatings on a six-color press predicted by laboratory tests," in: *TAPPI Coatings Conference Proceedings*, Montreal, Quebec, Canada, pp. 461-472.

Rousu, S., Gane, P., and Eklund, D. (2003). "Distribution of offset ink constituents in paper coating and implications for print quality," *TAPPI Journal* 4(7), 9-15.

SCAN P 70:09 (2009). "Papers and boards — Ink-absorbency value," Scandinavian Pulp, Paper and Board Testing Committee (SCAN).

Schmidt-Thümmes, J., Lawrenz, D., and Kröner, H. (2009). "Latex," in: *Pigment Coating and Surface Sizing of Paper (Papermaking Science and Technology, Vol. 11)*, J. Paltakari (ed.), Fapet Oy, Helsinki, Finland, pp. 207-225.

Shen, Z., Rajabi-Abhari, A., Oh, K., Lee, S., Chen, J., He, M., and Lee, H. L. (2021). "The effect of a polymer-stabilized latex cobinder on the optical and strength properties of pigment coating layers," *Polymers* 13(4), article 568. https://doi.org/10.3390/polym13040568

Ström, G. (2005). "Review: Interaction between offset ink and coated paper – A review of the present understanding," in: *Advances in Paper Science and Technology, Transactions of the XIIIth Fundamental Research Symposium*, Manchester, UK, pp. 1101-1137. DOI:10.15376/frc.2005.2.1101

TAPPI T 480 om-15 (2015). "Specular gloss of paper and paperboard at 75 degrees," TAPPI Press, Atlanta, GA, USA.

TAPPI T 555 (2015). "Roughness of paper and paperboard (Print-surf method)," TAPPI Press, Atlanta, GA, USA.

Van Gilder, R., Lee, O. J., Purfeerst, R., and Allswede, J. (1983). "High solids latexes for paper coatings," *TAPPI Journal* 66(11), 49-53.

Watanabe, J., and Lepoutre, P. (1982). "A mechanism for the consolidation of the structure of clay-latex coatings," *Journal of Applied Polymer Science* 27(11), 4207-4219. https://doi.org/10.1002/app.1982.070271112

Xu, R., Fleming, P. D., Pekarovicova, A., and Bliznyuk, V. (2005). "The effect of ink jet paper roughness on print gloss," *Journal of Imaging Science and Technology* 49(6), 660-666. https://doi.org/10.2352/J.ImagingSci.Technol.2005.49.6.art00016

Yoo, S. J., Cho, B. U., Kim, Y. S., Nam, B. K., Choi, S. M., and Lee, Y. K. (2007). "Effect of latex particle size, base paper grammage and coating color concentration on printing quality of coated paper," *Journal of Korea TAPPI* 39(4), 29-37.

Zang, Y. H., Du, J., Du, Y., Wu, Z., Cheng, S., and Liu, Y. (2010). "The migration of styrene butadiene latex during the drying of coating suspensions: When and how does migration of colloidal particles occur?," *Langmuir* 26(23), 18331-18339. https://doi.org/10.1021/la103675f

Article submitted: January 5, 2026; Peer review completed: March 21, 2026; Revised version received: March 23, 2026; Accepted: March 24, 2025; Published: March 26, 2026.
DOI: 10.15376/biores.21.2.4180-4197